Proceedings of the
44th IEEE Conference on Decision and Control, and
the European Control Conference 2005
Seville, Spain, December 12-15, 2005

Adaptive depth estimation in image based visual servo control of dynamic systems.

Robert Mahony and Arved von Brasch
Department of Engineering,
Australian National University,
ACT, 0200, AUSTRALIA.
mahony@ieee.org

Peter Corke
CSIRO, Manufacturing Science & Tech.,
Pullenvale, Queensland.
AUSTRALIA.
peter.corke@csiro.au

Tarek Hamel
I3S-CNRS
Nice-Sophia Antipolis,
FRANCE
thamel@i3s.unice.fr

***Abstract*— This paper considers the question of designing a fully image based visual servo control for a dynamic system. The work is motivated by the ongoing development of image based visual servo control of small aerial robotic vehicles. The observed targets considered are coloured blobs on a flat surface to which the normal direction is known. The theoretical framework is directly applicable to the case of markings on a horizontal floor or landing field. The image features used are a first order spherical moment for position and an image flow measurement for velocity. A fully non-linear adaptive control design is provided that ensures global stability of the closed-loop system.**

I. INTRODUCTION

With a range of applications in both the civilian and military fields, the development of automated aerial robots are an increasingly important field of robotics research. A key challenge in the development of autonomous aerial vehicles is to provide robust and simple sensing and control systems for local stabilisation. The core of this problem is the ability of the vehicle to measure its position and velocity relative to the local environment. Due to weight constraints the sensor input available to an aerial robot is severely limited. A common sensor suite includes an inertial measurement unit (IMU) and a camera. Although global positioning systems (GPS) are often integrated into a payload they tend to operate at too low a bandwidth (and do not function effectively indoors) to provide the key sensor input for localised stabilisation. In the framework of image based visual servo (IBVS) control, local environmental features are extracted as image points (or more general image features) from the video feed of the camera. These image features are used directly in a sensor based control strategy. For control of the full dynamic system, additional measurements are required. Recent work has lead to practical algorithms for determination of stable angular velocity and attitude estimates from low cost IMU units [14], [11]. Linear velocity measurements are the most difficult to obtain. One approach, motivated by insect behaviour [18], is to use visual flow information. Using visual flow directly in the control design fits with the philosophical paradigm of sensor based control design that has significant robustness advantages when dealing with low cost sensor systems [3]. Both visual flow and image feature measurements suffer from the lack of depth information inherent in measuring from a projection onto the image plane of a camera. Adaptive online estimation of the extrinsic calibration (relative position of camera to environment including 'depth') of a camera in visual servo control has been studied by a number of authors (cf. [17] and references therein). A key difficulty in applying adaptive techniques when the camera is mounted on the aerial platform is that the extrinsic calibration of the camera is dynamically evolving with the system.

In this paper, we consider the question of designing an image based visual servo (IBVS) control for a fully dynamic system. The motivating example is an aerial robotic system evolving on $SE(3)$, however, the key issues are addressed by considering just the linear translation dynamics of the system. The image feature considered is a first order unnormalised spherical moment [4], [1]. In addition, we use the sum of visual flow of the observed target points to provide a velocity estimate. An image based representation of the full dynamics of the system is derived and a control Lyapunov function is proposed for the closed-loop control design. Input actuation is dependent on an unmeasured depth parameter that varies dynamically with the system movement. This problem is overcome by proposing a modification to a standard input gain adaptive control strategy [8, pp. 168-173][13]. Lyapunov analysis is used to prove global asymptotic stability of the closed-loop system subject to continued observability of the targets. As a side effect of the control design the state estimate of the adaptive controller provides an approximate estimate of the dynamically changing depth. This approach has some resemblance to the early attempts to use adaptive control in IBVS schemes, however, we stress that this estimate is not used as a parameter in a certainty equivalence control design and the convergence of

0-7803-9568-9/05/$20.00 ©2005 IEEE

the closed-loop system does not require convergence of the depth estimate. Simulations are provided that demonstrate the performance of the closed-loop system.

II. Problem Formulation.

The motivating example considered is that of aerial robotic vehicles capable of quasi-stationary flight. The underlying system model considered in the sequel is based on those introduced in the literature to model the dynamics of helicopters [16], [2] and helicopter like vehicles [5], [12]

Let $\mathcal{A}$ denote the world frame and let $\mathcal{B}$ denote the body-fixed frame of vehicle airframe. The position of the airframe in the world frame is denoted $\xi = (x, y, z) \in \mathcal{A}$ and its attitude (or orientation) is given by a rotation $R : \mathcal{B} \to \mathcal{A}$. Let V (resp. Ω) denote the linear (resp. angular) velocity of the body expressed in the body fixed frame. Let m denote the total mass and $\mathbf{I}$ denote the inertia of the body. The dynamics of a rigid body are[1]:

$$\dot{\xi} = RV \tag{1}$$

$$m\dot{V} = -m\Omega \times V + F = -m\Omega_{\times}V + F \tag{2}$$

$$\dot{R} = R\Omega_{\times}, \tag{3}$$

$$\mathbf{I}\dot{\Omega} = -\Omega \times \mathbf{I}\Omega + \Gamma = -\Omega_{\times}\mathbf{I}\Omega + \Gamma. \tag{4}$$

The exogenous force and torque are denoted F and Γ respectively.

For a typical aerial robot capable of quasi-stationary flight the exogenous force may be modeled at a basic level by

$$F := -Te_3 + mgR^T e_3 \tag{5}$$

where $T \in \Re$ is a scalar input representing the thrust force applied in direction e_3. Motion in the linear dynamics (Eqn's 1 and 2) is obtained by specifying the thrust T and controlling the rotation $R(t)$ according to the attitude dynamics Eqn's 3 and 4.

In practice, it is possible to obtain accurate high bandwidth measurements of attitude and angular velocity directly from the IMU unit [14]. Based on this measurement a high gain feedback around the attitude loop is designed to regulate the force F. Following this approach, the linear translation dynamics, Eqn's 1 and 2, can be considered as a decoupled second order dynamic system with rate and saturation bounded input F. This simplification of the control design can be justified using small gain arguments [15]. It is an important simplification in the present paper, as it allows us to concentrate on issues associated with the image based control design without explicitly incorporating the additional complexities of the attitude dynamics in the control design. Thus, the dynamics considered are just Eqn's 1 and 2 subject to an unknown external disturbance Ω and with input $F \in \Re^3$.

[1]The notation $\Omega_{\times}$ denotes the skew-symmetric matrix such that $\Omega_{\times} v = \Omega \times v$ for the vector cross-product $\times$ and any vector $v \in \Re^3$.

The linear position and linear velocity cannot be derived from the low grade IMU systems used for non-military aerial robots. The IBVS control framework uses image features to replace the position state in Eq. 1. The conceptual extension of this idea to control of dynamic systems is to use visual flow to replace the velocity in Eq. 2. The resulting control problem involves a stabilisation of a set of non-linear dynamics expressed in terms of variables measured directly from the video feed of the onboard camera.

III. Image Dynamics

In this section, image plane kinematics and dynamics are derived for a first order un-normalised spherical moment image feature.

The target constellation considered consists of a finite set of disjoint points lying in a plane. The plane is termed the *target plane* and the image of the points are extracted in real-time by the vision system and passed to the control system as a sequence of 2D pixel locations $\{(X_i, Y_i)\}$. Assume that an accurate camera calibration matrix K is available. Each 2D centroid is transformed into a 3D point lying on a spherical image plane

$$p_i = \frac{\bar{p}_i}{|\bar{p}_i|}, \qquad \bar{p}_i = K \begin{pmatrix} X_i \\ Y_i \\ 1 \end{pmatrix}, \tag{6}$$

where $\bar{p}_i$ denotes the perspective projection of the ith 2D centroid. Let ${}^B P = (x_i, y_i, z_i) \in \mathcal{B}$ denote the actual target point lying on the target plane. Thus, $p_i = {}^B P / |{}^B P|$.

Since the camera is onboard the vehicle, the motion of the camera frame inherits dynamics in the body fixed frame. In order to simplify the derivation in the sequel, it is assumed that the camera fixed frame $\mathcal{C}$ coincides with the body fixed frame $\mathcal{B}$. The kinematics of the target point in the spherical image plane is given by

$$\dot{p}_i = -\Omega_{\times} p_i + \pi_{p_i} \frac{V}{|{}^B P_i|}. \tag{7}$$

where $\pi_{p_i} = I_3 - p_i p_i^T$ is the orthogonal projector onto the tangent space to the sphere at p_i.

Let η denote the unit normal to the target plane. Following the standard aeronautical conventions, the inertial frame is oriented such that gravity points in the positive E_z direction and the body-fixed frame is oriented in the same manner when the vehicle is in hover. Let $d := d(t)$, *depth*, denote the distance from the target surface to the origin of frame $\mathcal{B}$. Thus,

$$d(t) = -\langle {}^A\eta, \xi \rangle = |\langle {}^A\eta, \xi \rangle|$$

where ${}^A\eta$ denotes the normal direction in the inertial frame and $\langle \cdot, \cdot \rangle$ denotes the vector inner product. For each observed point p_i the depth may be calculated by

$$d(t) = \langle {}^B P_i, {}^B \eta \rangle = |{}^B P_i| \cos(\alpha_i)$$

where both P_i and η are expressed in the body-fixed-frame and α_i is the angle between the inertial direction η and the observed target point p_i. Thus, for all target points one has

$$|^B P_i| = \frac{d(t)}{\langle p_i, {}^B\eta \rangle} = \frac{d(t)}{\cos(\alpha_i)}.$$

Substituting this relationship into Eq. 7 yields

$$\dot{p}_i = -\mathrm{sk}(\Omega) p_i - \cos(\alpha_i)\pi_{p_i}\frac{V}{d(t)}. \tag{8}$$

The image feature used is the average landmark vector

$$q := \sum_{i=1}^{n} p_i \in \Re^3 \tag{9}$$

The image feature is essentially an un-normalised first order spherical moment. The image feature q contains three effective degrees of information and can be used as the basis of a position stabilisation control design [4].

Recalling Eq. 8, it may be verified that

$$\dot{q} = -\Omega \times q - Q\frac{V}{d(t)}, \tag{10}$$

where

$$Q = \sum_{i=1}^{i=n} \cos(\alpha_i)\pi_{p_i}. \tag{11}$$

Note that $Q := Q(t)$ is a time varying matrix that can be computed explicitly from observed image data. The matrix Q is not defined at target points since the angle α_i is not defined. In practice, as long as the camera remains above the target plane the matrix Q is always well defined. In Theorem 4.1 it is shown that $d(t) > 0$ along closed-loop solutions of the proposed control design. For two or more target points then $Q > 0$ is positive definite at all points except along the line containing the points. If there are three or more non-collinear targets then $Q > 0$ is positive-definite at all points in space, except for the target points themselves, where Q is not defined. On any bounded subset of the upper plane then the eigenvalues of Q are under-bounded $Q \geq \mu I_3$, where the constant μ depends on the bounded subset. As $\xi \to \infty$ then $\det Q \to 0$ due to the effective coalescence of the observed target points in the image.

The visual servo control task considered is that of position servo control of the camera frame above the image plane. The target pose is specified as a desired image feature q_*. In order, to obtain good passivity properties we assume that q_* is defined with respect to the inertial frame and inherits the ego motion of the camera [4]

$$\dot{q}_* = -\Omega_\times q_*$$

This requires that we have access to an inertial direction in the body-fixed-frame. In the sequel we will use the direction η normal to the image plane that will also be the gravitational direction.

The image based error considered is the difference between the measured centroid and the target vector expressed in the camera fixed frame

$$\delta := q - q_*. \tag{12}$$

In earlier work [4] it has been shown that for two or more non-collinear targets then $q = q_*$ uniquely defines a position $\xi = \xi_*$ in Cartesian space.

Deriving δ yields:

$$\dot{\delta} = -\Omega_\times \delta - Q\frac{V}{d(t)} \tag{13}$$

The above equation (Eq. 13) defines the kinematics of the visual error δ. It is of interest to study the structural properties of Eq. 13. Consider the storage function $|\delta|^2$. The derivative of this function is

$$\frac{d}{dt}|\delta|^2 = -\delta^T \Omega_\times \delta - \delta^T Q\frac{V}{d(t)}.$$

The first term is zero due to the skew symmetry of Ω. Since the matrix $Q > 0$ is positive definite, the second term can be seen as an inner product between δ and $V/d(t)$. The second term acts as a supply function to the storage function $|\delta|^2$. Choosing $V = Q^{-1}\delta$ acts to decrease $|\delta|^2$ in proportional rate to the unknown depth $d(t) > 0$. Since $d(t)$ is positive in the expected flight regime the kinematic control proposed is likely to be effective in stabilising the closed-loop system. In earlier work [4] the authors used this approach in a backstepping control to obtain control of the full dynamics Eqn's 1-4 of the vehicle. However, this approach requires a measurement of the velocity V and cannot be used in the present approach.

The visual velocity measure that is used is

$$W(t) = \frac{V(t)}{d(t)} \tag{14}$$

To measure $W(t)$ from the image sequence requires a differentiation of the image feature $q(t)$. Formally, one has

$$W(t) = -Q^{-1}\left(\dot{q} + \Omega \times q\right).$$

Clearly, the derivative $\dot{q}$ must be estimated using a finite difference process running at frame rate and the dependence on the angular velocity will based on reading from the IMU. It is interesting to note that $W(t)$ may be written as

$$W(t) = -Q^{-1}\sum_{i=1}^{n}\left(\dot{p}_i + \Omega \times p_i\right) = -Q^{-1}\sum_{i=1}^{n} X_t(p_i)$$

The bracketed term, equated to $X_t(p_i)$, is the spherical visual flow for each target point p_i. Thus, the velocity estimate $W(t)$ is a scaled average visual flow of the target points.

In order to obtain a full image based representation of the system dynamics it is necessary to compute the dynamic

response of $W(t)$ induced by the system dynamics Eqn's 1 and 2. Differentiating $W(t)$ one obtains

$$\begin{aligned}\dot{W} &= \frac{\dot{V}}{d} - \frac{V\dot{d}}{d^2} \\ &= -\Omega \times W + W\langle W, \eta\rangle + \frac{1}{d(t)}\frac{F}{m} \end{aligned} \tag{15}$$

where

$$\dot{d} = -\langle \eta, V\rangle = -d\langle \eta, W\rangle \tag{16}$$

Thus, the full dynamic equations of the system expressed in the image plane features are Eqn's 13 and 15. All variables in the equations are related to the measured values δ, $W(t)$ and Ω. The dynamics depend on an unknown and time-varying input gain $1/d(t)$.

IV. Control Design

In this section a stabilising control design for the system Eqn's 13 and 15 is proposed.

The control problem considered is to develop a control F that stabilises $\delta \to 0$ given the dynamic system

$$\dot{\delta} = -\Omega_\times \delta - QW \tag{17}$$

$$\dot{W} = -\Omega \times W + W\langle W, \eta\rangle + \frac{F}{md(t)} \tag{18}$$

$$\dot{d} = -d\langle \eta, W\rangle \tag{19}$$

with all variables measured except $d(t)$. It is necessary to incorporate a model of the dynamic response of $d(t)$ into the control design. Let $\hat{d}(t)$ denote an estimate of $d(t)$. The estimate $\hat{d}(t)$ is given dynamics based on those of $d(t)$

$$\dot{\hat{d}}(t) = -\hat{d}\langle \eta, W\rangle, \qquad \hat{d}(0) = \hat{d}_0. \tag{20}$$

Note that the dynamics of $\hat{d}$ depend only on known variables and may be computed on-line. Moreover, if $\hat{d}_0 = d(0)$ then in principal $d(t) = \hat{d}(t)$ for all $t \geq 0$. Consider the ratio $\hat{d}(t)/d(t)$. One has

$$\frac{d}{dt}\left(\frac{\hat{d}}{d}\right) = \frac{\dot{\hat{d}}}{d} - \frac{\hat{d}\dot{d}}{d^2} = -\frac{\hat{d}\langle \eta, W\rangle}{d} + \frac{\hat{d}d\langle \eta, W\rangle}{d^2} = 0$$

Integrating this relationship over time one obtains

$$\hat{d}(t)/d(t) = a$$

where a is an unknown constant. Substituting into Eq. 15 one obtains

$$\dot{W} = -\Omega \times W + W\langle W, \eta\rangle + a\frac{F}{m\hat{d}(t)} \tag{21}$$

The purpose of this manipulation is that the resulting dynamics in W depend on an unknown *constant* parameter a. The control term $F/(m\hat{d}(t))$ can be directly computed from the value of $\hat{d}(t)$ obtained from the integration of Eq. 20 in the control architecture. Note that the initial condition $\hat{d}_0$ need not be correct as the proposed control design will adapt a to compensate for the error in the initial condition.

The control design is a direct application of standard adaptive control design techniques to Eqn's 17 and 21. Introduce notation $\rho = 1/a$ for the inverse of the control gain a. Let $\hat{\rho}(t)$ be an adaptive estimate of the constant ρ. Define

$$\tilde{\rho} = \rho - \hat{\rho}$$

Let $k > 0$ be a positive (kinematic gain) constant and define the velocity error

$$\epsilon = W - k\delta$$

Theorem 4.1: Consider the system Eqn's 1 and 2 and its expression in terms of image error kinematics and dynamics, Eqn's 17 and 21 along with unmeasured depth dynamics Eq. 16. Assume that the observed target consists of at least three non-collinear points. Assume $d(0) > 0$ and that the goal q_* corresponds to a positive depth. Let $k, \sigma, c, \lambda, > 0$ be positive gains corresponding to the kinematic, k and σ, dynamic, c, and adaptation, λ, closed-loop system responses. Let $\hat{\rho}$ denote an estimate of the inverse of the unknown input gain $\rho = 1/a$. For an arbitrary estimate $\hat{d}_0 > 0$ of the initial height set

$$\dot{\hat{d}}(t) = -\hat{d}\langle \eta, W\rangle, \qquad \hat{d}(0) = \hat{d}_0.$$

Define the control input and adaptation law by

$$\begin{aligned} U &:= \sigma Q\delta - W\langle W, \eta\rangle - kQW - c\epsilon, \\ F(t) &:= \hat{\rho} m\hat{d}(t) U, \end{aligned} \tag{22}$$

$$\dot{\hat{\rho}} := -\lambda\langle U, \epsilon\rangle, \qquad \hat{\rho}(0) = 1. \tag{23}$$

Define a Lyapunov function $\mathcal{L}$ by

$$\mathcal{L} = \frac{\sigma}{2}|\delta|^2 + \frac{1}{2}|\epsilon|^2 + \frac{a}{2\lambda}|\tilde{\rho}|^2$$

Then, the closed-loop trajectory exists for all time and satisfies

$$d(t) > 0.$$

There exists $\mu_0 > 0$, that depends on the initial conditions of the system, such that along closed-loop solutions of the system

$$\frac{d}{dt}\mathcal{L} = -k\sigma\delta^T Q\delta - c|\epsilon|^2, \qquad Q(t) > \mu_0 I.$$

The error terms δ, ϵ are convergent to zero and the system is globally asymptotically stable to ξ_* with domain $d > 0$. The parameter estimate error is convergent ($\tilde{\rho} \to$ const.).

Proof: The control and adaptation laws are well defined and smooth for $d > 0$. From classical ODE theory the closed-loop solutions either exist for all time, or there exists a first

time $T > 0$, such that $d(T) = 0$, for which the solutions exist for all time $t < T$. For $t < T$, differentiating $\mathcal{L}$ yields

$$\dot{\mathcal{L}} = -\sigma\langle\delta, \Omega_\times\delta\rangle - \sigma\langle\delta, QW\rangle - \frac{a\tilde{\rho}\dot{\hat{\rho}}}{\lambda} + \left\langle \epsilon, -\Omega \times W + W\langle W, \eta\rangle + a\frac{F}{m\hat{d}(t)} + k\Omega_\times\delta + kQW \right\rangle$$

The term $\langle\delta, \Omega_\times\delta\rangle = 0$ due to the anti-symmetric of $\Omega_\times$. Combining terms, substituting for F and $\dot{\hat{\rho}}$, $\hat{\rho} = \rho - \tilde{\rho}$, and recalling that $Q = Q^T$ is symmetric yields

$$\dot{\mathcal{L}} = -k\sigma\langle\delta, Q\delta\rangle - c\langle\epsilon, \epsilon\rangle.$$

This proves that $\mathcal{L}(t) \leq \mathcal{L}(0)$ and by construction that $|\xi(t)| \leq B$ for some $B > 0$. Since the target has at least three non-collinear points then it follows that $Q(\xi) > 0$ on the ball $|\xi| \leq B$, $d \geq 0$. Note that Q is not defined at target points, however, its eigenvalues in all points around a target point are bounded away from zero. It follows that there exists a constant μ_0 such that $Q(t) > \mu_0 I$ as long as the closed-loop solution is well defined.

Consider the closed-loop dynamics of $d(t)$. Since $\mathcal{L}(t) < \mathcal{L}(0)$ then

$$|W(t)| \leq |\epsilon| + k|\delta| \leq A\sqrt{\mathcal{L}(0)}$$

for some constant $A > 0$. This implies that

$$|V(t)| \leq A\sqrt{\mathcal{L}(0)}d(t)$$

and

$$\dot{d} = -\langle\eta, V\rangle \geq -|\eta|\,|V| \geq -A\sqrt{\mathcal{L}(0)}d(t)$$

It follows that $d(t) \geq d(0)\exp(-tA\sqrt{\mathcal{L}(0)})$ and $d(t) > 0$ for all $t \leq \infty$. As a consequence the closed-loop solutions exists for all time.

Finally, since $Q > \mu_0 I$ is positive-definite and the closed-loop solutions are bounded and exist for all time, then applying Lyapunov's method [15] proves global asymptotic stability of δ and ϵ to zero. Note that $\delta = \epsilon = 0$ implies that $W = 0$. Since $\dot{\mathcal{L}} \leq 0$ then $\mathcal{L}$ is monotonic and converges to a minimum $\mathcal{L}_\infty = \frac{1}{2}|\tilde{\rho}_\infty|^2$. Applying Barbalat's lemma [7, Th. 4.8] proves convergence of $\dot{\hat{\rho}} \to 0$ and $\hat{\rho}(t)$ converges to a constant. The global convergence of the result follows from the uniqueness of the minimal point of the cost $|\delta|^2$ established in [4]. ■

Note that the derivative of the Lyapunov function is independent of the unknown error term $\tilde{\rho}$. This is typical of adaptive control algorithms of the form proposed. For the particular control task considered, $W \to 0$ with convergence of the control errors $\epsilon, \delta \to 0$, and as a consequence one *cannot* apply LaSalles principal [15] to infer convergence of the asymptotic value of $\tilde{\rho}$. Indeed, if the system is correctly positioned at time zero but $\hat{d}_0 \neq d(0)$ then $\epsilon = \delta = W = 0$ for all time and $\tilde{\rho} = d(0)/\hat{d}_0 - 1$ for all time. This is an important aspect of the control design proposed, it is not necessary to accurately reconstruct the Cartesian depth of the target. The approximate reconstruction undertaken provides sufficient information to guarantee the convergence of the closed-loop system.

Remark 4.2: It is possible to extend the above control design to incorporate a time varying goal $q_\star = q_\star(t)$ using a similar approach to that used in Mahony and Hamel [9]. In 'this case the asymptotic value of $W(t) \not\to 0$ and convergence of the parameter $\hat{\rho} \to \rho$ can be guaranteed using a persistence of excitation argument. △

An attractive aspect of the control design is that the velocity feature W inherits important properties of visual flow based control algorithms. Since W is related to the visual flow field of the target it is singular, $W \to \infty$, as $d \to 0$. In practice, this ensures that the closed-loop system is highly sensitive to velocity errors when it is close to the target plane and less sensitive as the depth increases. This is an important property for aerial robots. It is the physical reason that it is possible to prove $d(t) > 0$ along closed-loop trajectories of the system in Theorem 4.1. This is an example of a situation where working with the visual measure has advantages for the closed-loop response of the system.

A second advantage of the control proposed is that the kinematic error is bounded

$$|\delta| = |q - q_*| \leq \sum |p_i| + |q_*| \leq n + |q_*|.$$

As a consequence, the kinematic demand is bounded in the control design. In practice, this does not effect the local convergence of the system, however, for initial conditions far from the set point the velocity demand is bounded. Thus, for large initial errors the closed-loop trajectory resembles a rate bounded time optimal trajectory, where, in the initial phase (after acceleration) the vehicle travels at a constant pace toward the goal, and then, as it approaches the goal and the rate saturation is no longer active, it decelerates and converges to the set point. This aspect of the dynamic response is desirable for the closed-loop response of aerial robotic vehicles.

V. Simulation results

In this section we present a simulation study of the proposed control design. An example trajectory is considered that is representative of the closed-loop response over a wide range of initial conditions.

Simulations were undertaken in the SIMULINK environment based on the MATLAB package. An advantage of the SIMULINK environment is that it allows multirate simulations. A separate block was coded for the full rigid-body dynamics of the UAV. The UAV dynamics are simulated as continuous-time dynamics (computed using SIMULINK ODE integration procedures). Following the assumptions of the paper, position dynamics of the system are decoupled from the attitude dynamics and the attitude dynamics were

not actuated in the simulation. The camera was also modelled as a separate discrete time SIMULINK block operating at 25Hz. The visual flow is computed at 25Hz based on a simple first order differencing scheme and both the image features are passed to the control scheme as zero-order hold signals. The control law is modelled as a continuous-time process. This is based on the idea that the practical implementation of the control would be undertaken at a sufficiently fast rate to ignore the sample hold effects.

A set of initial conditions that were found to be illustrative of the system response were taken to be

$$(x, y, z) = (2, 1.5, -3)$$

An initial estimate of depth $\hat{d}(0) = 2$ was used. The true initial depth was $d(0) = 3$ creating an initial error in the depth estimation. The initial condition for the estimate $\hat{\rho}(0) = 1$ as specified in the control algorithm. The goal feature was specified to be

$$q_* = (0, 0, 3.8806).$$

This corresponds to a goal position of $(0, 0, -1)$ for a target configuration with 4 targets symmetrically arranged around the origin at a radius of 0.25m. The airframe was chosen to have a mass of 1kg and inertia of $0.125 I_3$ kg.m^2.

The following controller gain parameters were chosen

$k = 0.005$	$\lambda = 0.5$
$c = 0.1$	$\sigma = 0.005$

Tuning the gains on an adaptive control design of this complexity is a difficult business. The principal kinematic gains k and σ are chosen equal as they both represent exponential rates of convergence in the primary kinematic coordinates. The values were chosen experimentally to obtain a system settling time of around 60 seconds. The adaptive, λ, and dynamic, c, gains were tuned together. The goal of the adaptive gain tuning was to obtain a settling time of the $\hat{\rho}$ dynamics of around 60 seconds, the same time frame as the (x, y) dynamics. The dynamic gain c was adjusted to obtain the approximate %30 overshoot seen in the dynamics response of the x and y coordinates. Tuning the two gains iteratively lead to the gain choices shown. A final important modification to the control presented in section IV is the inclusion of an inverse estimate of the image Jacobian in the control design. This modification of the control design is done to balance the rates of convergence in the (x, y) and z directions due to the low sensitivity of the image feature to change in depth at the set point for the camera geometry considered. This is a standard process in image based visual servo control [3]. The final applied control varies from that proposed in Theorem 4.1 only in the definition of ϵ and U,

$$\begin{aligned} \epsilon_{\text{mod}} &:= W - kQ_0^{-1}\delta, \\ U_{\text{mod}} &:= \sigma Q\delta - W\langle W, \eta\rangle \\ &\quad - kQ_0^{-1}QW - c\epsilon - k[Q_0^{-1}, \Omega_\times]\delta. \end{aligned}$$

Here Q_0 (a constant matrix) is the estimate of Q at the goal configuration. The term $[Q_0^{-1}, \Omega_\times] = Q_0^{-1}\Omega_\times - \Omega_\times Q_0^{-1}$ is a compensation that is needed due to the loss of passivity in the derivative of $|\epsilon_{\text{mod}}|^2$ with the introduction of the scaling factor.

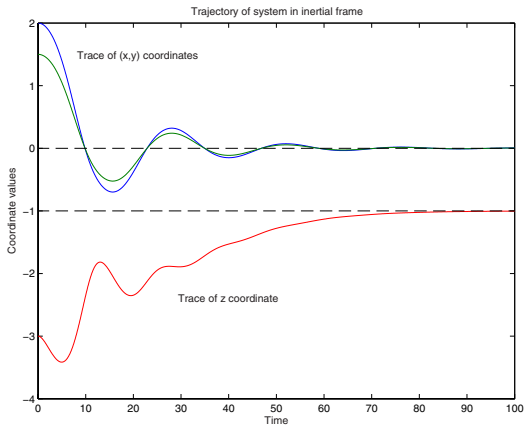

Fig. 1. Inertial trajectory of closed-loop system

The results obtained demonstrate the effective performance of the control algorithm. Figure 1 shows the desired stable convergence of the (x, y) and z coordinates. Note that the z dynamics first demonstrate a movement away from the desired set point. This is a characteristic of visual servo algorithms using the image features considered. Due to the low damping of the system this generates a damped oscillatory response in the depth dynamics that is clearly shown in Figure 2. In Figure 2 it is interesting to observe the effective tracking of the two signals. The two traces appears to approach each other as the depth decreases. This is due to the relationship $\hat{d}(t) = ad(t)$. This property is also linked to the fact that the depth can never reach zero during evolution of the closed-loop system.

The evolution of the adaptive parameter is typical of adaptive algorithms of this type, Figure 3 . It is interesting to note that $\hat{\rho} \not\to 2/3 = 1/a$, however, as discussed in Section IV, this does not effect the overall convergence of the algorithm. The convergence of the Lyapunov function, Figure 4 demonstrates the overall stability of the algorithm.

VI. Conclusions

In this paper we have presented a novel adaptive control design for image based visual servo control of dynamic systems. The key contribution of the paper, is incorporating visual flow and image based features together to get an image based, dynamic model of a system, and the application of extended matching techniques to obtain a rigorous adaptive control design for the stabilization problem. If desired, it is possible to extend the proposed approach to incorporate the attitude dynamics by using the extended matching approach

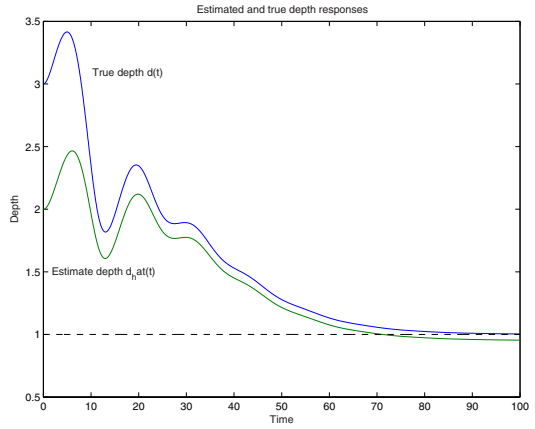

Fig. 2. Time evolution of the true depth $d(t)$ and the controller parameter $\hat{d}(t)$

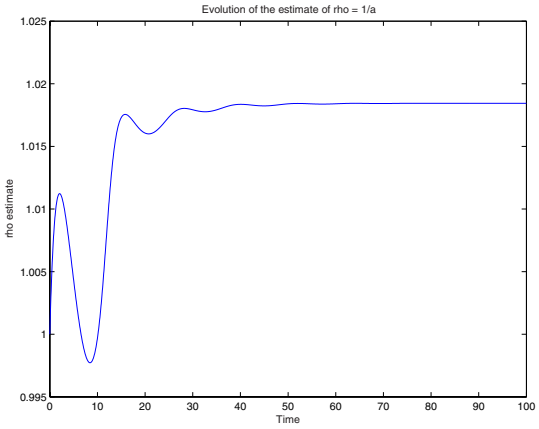

Fig. 3. Time evolution of adaptive estimate $\hat{\rho}$ of ρ.

[8], [13] similar to the manner undertaken in the reference [10].

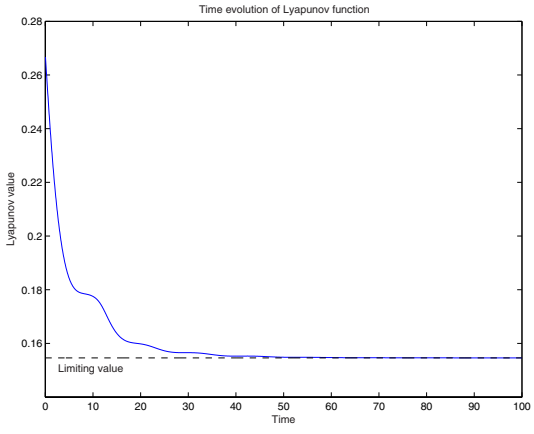

Fig. 4. Time evolution of the Lyapunov function.

REFERENCES

[1] F. Chaumette. Image moments: a general and useful set of features for visual servoing. *IEEE Transactions on Robotics*, 20(4):713–723, 2004.

[2] M. Dahlen E. Frazzoli and E. Feron. Trajectory tracking control design for autonomous helicopters using a backstepping algorithm. *Proceedings of the American Control Conference ACC*, pages 4102–4107, 2000.

[3] B. Espiau, F. Chaumette, and P. Rives. A new approach to visual servoing in robotics. *IEEE Transactions on Robotics and Automation*, 8(3):313–326, 1992.

[4] T. Hamel and R. Mahony. Visual servoing of an under-actuated dynamic rigid-body system: An image based approach. *IEEE Transactions on Robotics and Automation*, 18(2):187–198, April 2002.

[5] T. Hamel, R. Mahony, R. Lozano, and J. Ostrowski. Dynamic modelling and configuration stabilization for an X4-flyer. In *Proceedings of the International Federation of Automatic Control Symposium, IFAC 2002*, Barcelona, Spain, 2002.

[6] R. Kelly, J. Moreno, and R. Campa. Visual servoing of planar robots via velocity fields. In *43rd IEEE Conference on Decision and Control*, pages 4028–4033, Atlantis, Paradise Island, Bahama, December 2004.

[7] H. K. Khalil. *Nonlinear Systems*. Prentice Hall, New Jersey, U.S.A., second edition, 1996.

[8] M Krstic, I Kanellakopoulos, and P V Kokotovic. *Nonlinear and Adaptive Control Design*. American Mathematical Society, Providence, Rhode Island, U.S.A., 1995.

[9] R. Mahony and T. Hamel. Stable tracking control for unmanned aerial vehicles using non-inertial measurements. In *Proceedings of the Conference on Decision and Control, CDC'2000*, pages 2971–2976, Sydney, N.S.W., Australia, 2000.

[10] R. Mahony and T. Hamel. Adaptive compensation of aerodynamic effects during takeoff and landing manoeuvres for a scale model autonomous helicopter. *European Journal of Control*, 7(1), 2001.

[11] R. Mahony, T. Hamel, and Jean-Michel Pflimlin. Complimentary filter design on the special orthogonal group $so(3)$. In *Proceedings of the IEEE Conference on Decision and Control, CDC05*, Seville, Spain, December 2005. Institue of Electrical and Electronic Engineers.

[12] P. Pounds, R. Mahony, P. Hynes, and J. Roberts. Design of a four-rotor aerial robot. In *Australasian Conference on Robotics and Automation Conference, ACRA-2002*, Auckland, New Zealand, 2002.

[13] L. Praly, G. Bastin, J.-B. Pomet, and Z. Jiang. *Adaptive stabilization of non-linear systems*, pages 347–434. Springer-Verlag, Berlin, 1991.

[14] J. Roberts, P. Corkes, and G. Buskey. Low-cost flight control system for a small autonomous helicopter. In *Proceedings of the Australasian Conference on Robotics and Automation, ACRA02*, Auckland, New-Zealand, 2002.

[15] R Sepulchre, M Janković, and P Kokotović. *Constructive Nonlinear Control*. Springer-Verlag, London, 1997.

[16] O. Shakernia, Y. Ma, T. J. Koo, and S. Sastry. Landing an unmanned air vehicle: vision based motion estimation and nonlinear control. *Asian Journal of Control*, 1(3):128–146, 1999.

[17] Yantao Shen, Dong Sun, Yun-Hui Liu, and Kejie Li. Asymptotic trajectory tracking of manipulators using uncalibrated visual feedback. *IEEE/ASME Trasnactions on Mechatronics*, 8(1):87–98, 2003.

[18] M. Srinivasan, J. Chahl, K. Weber, S. Venkatesh, M. Nagle, and S. Zhang. Robot navigation inspired by principles of insect vision. *Robotics and Autonomous Systems*, 26:203–216, 1999.